Life Sciences 310 (2022) 121114

Contents lists available at ScienceDirect

Life Sciences

journal homepage: www.elsevier.com/locate/lifescie

15-keto-Prostaglandin E_2 exhibits bioactive role by modulating glomerular cytoarchitecture through EP2/EP4 receptors

Aikaterini Kourpa [a,b], Debora Kaiser-Graf [b], Anje Sporbert [c], Aurélie Philippe [d,e], Rusan Catar [d], Michael Rothe [f], Eva Mangelsen [b], Angela Schulz [b], Juliane Bolbrinker [b], Reinhold Kreutz [b], Daniela Panáková [a,*]

[a] Max Delbrück Center for Molecular Medicine in the Helmholtz Association, Buch, Berlin, Germany
[b] Charité-Universitätsmedizin Berlin, Corporate member of Freie Universität Berlin, Humboldt-Universität zu Berlin, and Berlin Institute of Health, Institute of Clinical Pharmacology and Toxicology, Berlin, Germany
[c] Max Delbrück Center for Molecular Medicine in the Helmholtz Association, Advanced Light Microscopy, Buch, Berlin, Germany
[d] Charité-Universitätsmedizin Berlin, Corporate member of Freie Universität Berlin, Humboldt-Universität zu Berlin, and Berlin Institute of Health, Department of Nephrology and Medical Intensive Care, Berlin, Germany
[e] Berlin Institute of Health, Charité-Universitätsmedizin Berlin, BIH Biomedical Innovation Academy, Berlin, Germany
[f] Lipidomix GmbH, Berlin, Germany

ARTICLE INFO

Keywords:
Prostaglandins
15-keto-PGE_2
EP receptors
Zebrafish
Podocytes
Glomerular vascularization

ABSTRACT

Aims: Prostaglandins are important signaling lipids with prostaglandin E_2 (PGE_2) known to be the most abundant prostaglandin across tissues. In kidney, PGE_2 plays an important role in the regulation of kidney homeostasis through its EP receptor signaling. Catabolism of PGE_2 yields the metabolic products that are widely considered biologically inactive. Although recent *in vitro* evidence suggested the ability of 15-keto-PGE_2 (a downstream metabolite of PGE_2) to activate EP receptors, the question whether 15-keto-PGE_2 exhibits physiological roles remains unresolved.

Materials and methods: Pharmacological treatment was performed in transgenic zebrafish embryos using 500 μM 15-keto-PGE_2 and 20 μM EP receptors antagonists' solutions during zebrafish embryonic development. After the exposure period, the embryos were fixed for confocal microscopy imaging and glomerular morphology analysis.

Key findings: Here, we show that 15-keto-PGE_2 can bind and stabilize EP2 and EP4 receptors on the plasma membrane in the yeast model. Using lipidomic analysis, we demonstrate both PGE_2 and 15-keto-PGE_2 are present at considerable levels in zebrafish embryos. Our high-resolution image analysis reveals the exogenous treatment with 15-keto-PGE_2 perturbs glomerular vascularization during zebrafish development. Specifically, we show that the increased levels of 15-keto-PGE_2 cause intercalation defects between podocytes and endothelial cells of glomerular capillaries effectively reducing the surface area of glomerular filtration barrier. Importantly, 15-keto-PGE_2-dependent defects can be fully reversed by combined blockade of the EP2 and EP4 receptors.

Significance: Altogether, our results reveal 15-keto-PGE_2 to be a biologically active metabolite that modulates the EP receptor signaling *in vivo*, thus playing a potential role in kidney biology.

1. Introduction

The human kidney consists of about a million of nephrons that comprise the basic structural and functional unit of the kidney [1–3]. Each nephron contains a glomerulus, the main blood filtration apparatus, a system of proximal and distal tubules, the loop of Henle, as well as the collecting duct, which are responsible for the nutrients, water and ions reabsorption, the maintenance of the normal fluid flow, and the concentration and excretion of the urine [1,3,4]. The glomerulus contains various specialized cells responsible for forming the capillaries network and the glomerular filtration barrier (GFB), the principal blood filtration system. The GFB consists of podocytes, the glomerular basement membrane (GBM) and the fenestrated endothelium [5,6]. In physiological conditions the GFB demonstrates relative impermeability to proteins with molecular weight above 70 kDa and other macromolecules, therefore prevents the excretion of blood cells and large proteins

* Corresponding author.
E-mail address: daniela.panakova@mdc-berlin.de (D. Panáková).

https://doi.org/10.1016/j.lfs.2022.121114
Received 22 August 2022; Received in revised form 6 October 2022; Accepted 17 October 2022
Available online 20 October 2022

into the urine [7]. Upon damage of the GFB, its permeability to the molecules of increasing size is affected resulting in the presence of molecules like albumin or larger in the urine, a pathological condition known as albuminuria [7,8].

Despite the distinct differences between fish and mammals in the formation and/or function of kidney arising most notably from the diverse living environment *i.e.* terrestrial *versus* aquatic, the human nephron shares a similar segmentation pattern with the zebrafish embryonic kidney (pronephros) [9] thus rendering the latter as an important model for studying kidney development and physiology as well as various forms of renal diseases [10–13]. The developing zebrafish pronephros consists of two nephrons with bilateral glomeruli, kidney tubules and a collecting duct [11,14]. In zebrafish, the onset of glomerular filtration takes place at 48 hours post fertilization (hpf), while the glomerular capillarization and the formation of the GFB is completed by 72 hpf [9,14,15].

Prostaglandins (PG) including PGE_2, PGF_{2a} and PGD_2, are important active lipid mediators synthesized from arachidonic acid (AA) with the participation of cyclooxygenases 1 and 2 (COX1, COX2) and specialized prostaglandin synthases [16,17]. They have been found in almost every tissue in humans as well as other vertebrates. Several reports highlight their crucial role in both physiological and pathological conditions including inflammatory response, cancer, homeostasis regulation, hematopoiesis, and kidney physiology [18–25]. Among them, prostaglandin E_2 (PGE_2) is the most abundant prostaglandin in various organs including the kidney, where the role of PGE_2 has been extensively studied in the past years [17,25,26]. PGE_2 contributes to the normal renal physiology as well as pathogenic mechanisms underlying the initiation and progression of chronic kidney disease (CKD) [17,27].

PGE_2 acts through its four G-protein–coupled prostaglandin receptors (EP): EP1, EP2, EP3 and EP4 [28,29]. Recently, we showed that combined EP2 and EP4 signaling is important for autocrine PGE_2 activation in human podocytes [30]. Thus, these receptors could be important targets for the development of therapeutic strategies against multiple renal complications ascribed to prostaglandin signaling [17,25–27,31]. The catabolism of PGE_2 involves two steps [32] (Fig. 1a). The first and also rate-limiting step is catalyzed by 15-prostaglandin dehydrogenase (15-PGDH) and results in the synthesis of 15-keto-PGE_2 [32]. The enzyme that catalyzes the second step of the complete PGE_2 inactivation is prostaglandin reductase (PTGR or Δ^{13}-PG-Reductase) and yields 13,14-dihydro-15-keto-PGE_2 [32,33]. Until recently, these catabolic products, 15-keto-PGE_2 and 13,14-dihydro-15-

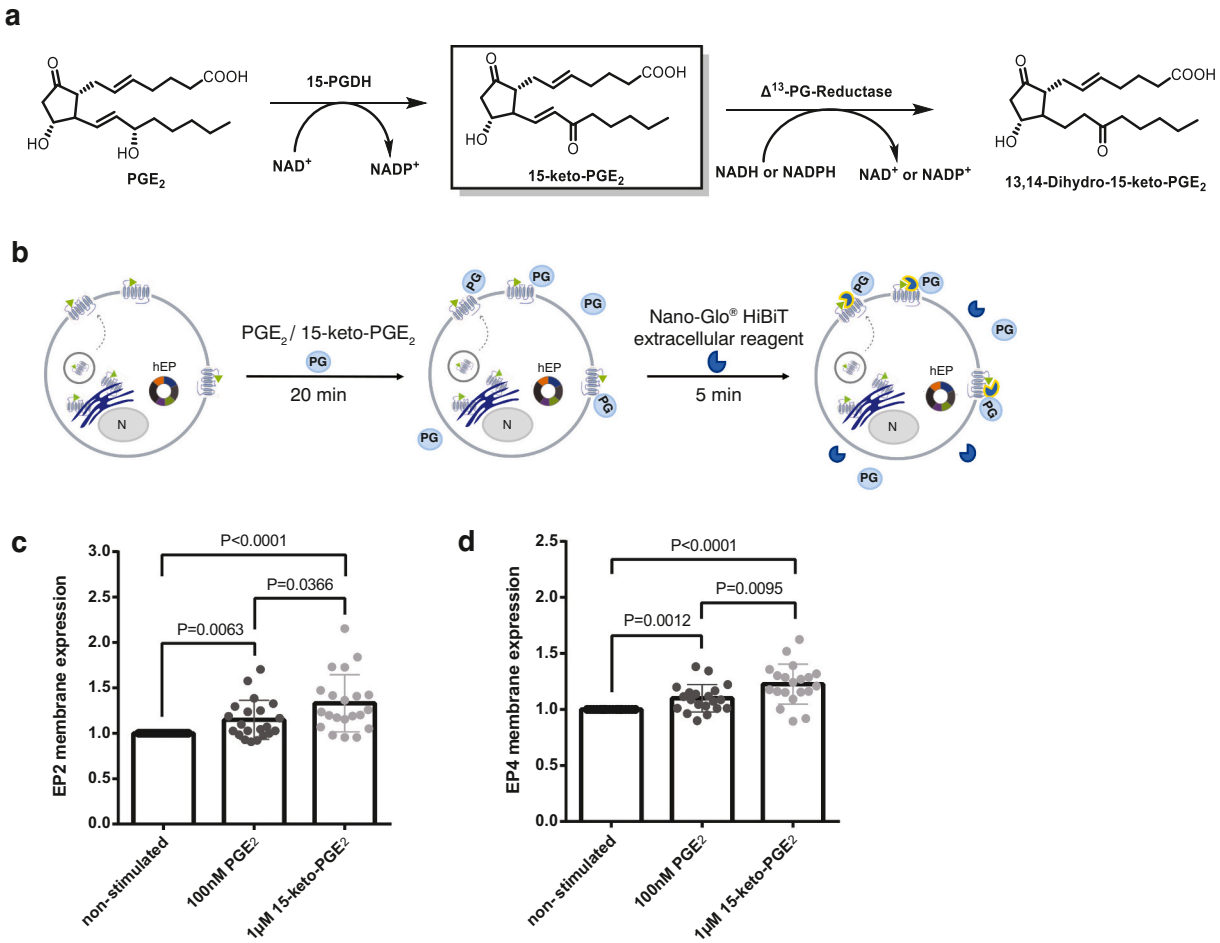

Fig. 1. 15-keto-PGE_2 binds EP receptors *in vitro*. (a) PGE_2 degradation pathway highlighting the first synthesized metabolic product, 15-keto-PGE_2. (b) Schematic of the experimental assay to measure receptor membrane expression using the Nano-Glo® HiBiT Extracellular Detection System. The HiBiT-tagged receptor is synthesized, processed and released from the endoplasmic reticulum (ER) and transported by secretory vesicles to the cell membrane. Yeast expressing HiBiT-tagged hEP2 or HibiT-tagged hEP4 receptors on the membrane were stimulated with either 100 nM PGE_2, 1 μM 15-keto-PGE_2 or equal volume of medium for non-stimulated controls for 20 min to allow ligand binding. Adding of Nano-Glo® HiBiT Extracellular Reagent (containing Buffer, substrate and LgBiT protein) generated luminescence by structural complementation of LgBiT proteins with extra-cellular displayed HiBiT-tags, and thus allowing quantification of the number of receptors in the membrane; N represents cell nucleus. Quantification graphs of the (c) HiBiT-tagged hEP2 and (d) HiBiT-tagged hEP4 receptors cell membrane expression after 20 min stimulation with PGE_2 (dark grey) and 15-keto-PGE_2 (light grey). Wilcoxon test and Mann-Whitney tests were performed. Values are plotted as mean ± SD; $P < 0.05$ considered significant.

keto-PGE_2, were widely considered as biologically inactive [32,34]. Latest *in vitro* studies have, however, suggested that 15-keto-PGE_2 can activate the production of cAMP *via* EP receptors [35], and may act as a partial agonist of EP2, taking over the signaling roles of PGE_2 [36]. In addition, new evidence indicates 15-keto-PGE_2 is able to stimulate peroxisome proliferator-activated receptor gamma (PPAR-γ) in various models [37–39]. Importantly, the physiological importance of the PGE_2 metabolites, and specifically, 15-keto-PGE_2, in the kidney biology and its potential to activate EP receptors *in vivo* remains unresolved.

Here, we use the yeast model expressing human EP2 (hEP2) and EP4 (hEP4) receptors and the developing zebrafish kidney to examine the signaling potential of 15-keto-PGE_2. We investigate whether 15-keto-PGE_2 is capable of stimulating the EP receptors *in vivo* and further elucidate the potential role of prostaglandin catabolic pathway in kidney biology with the focus on GFB formation and function.

2. Results

2.1. 15-keto-PGE_2 binds EP2 and EP4 receptors in vitro

Although recent *in vitro* studies demonstrated 15-keto-PGE_2, the metabolic product synthesized during the PGE_2 inactivation (Fig. 1a), is able to stimulate G-protein-coupled EP receptors [35,36], its prospective signaling role is not fully resolved. To better understand the interaction between 15-keto-PGE_2 and the EP receptors, we used the Nano-Glo® HiBiT extracellular detection system (see Material and methods for details) applied in the yeast model, in which the single GPCR of the yeast (MMY28 strain) [40] was replaced upon transformation to express individually HiBiT-tagged human EP2 (hEP2) and EP4 (hEP4) receptors (Fig. 1b). This system allowed us to quantify the relative membrane expression of hEP2 and hEP4 receptors before and after prostaglandin

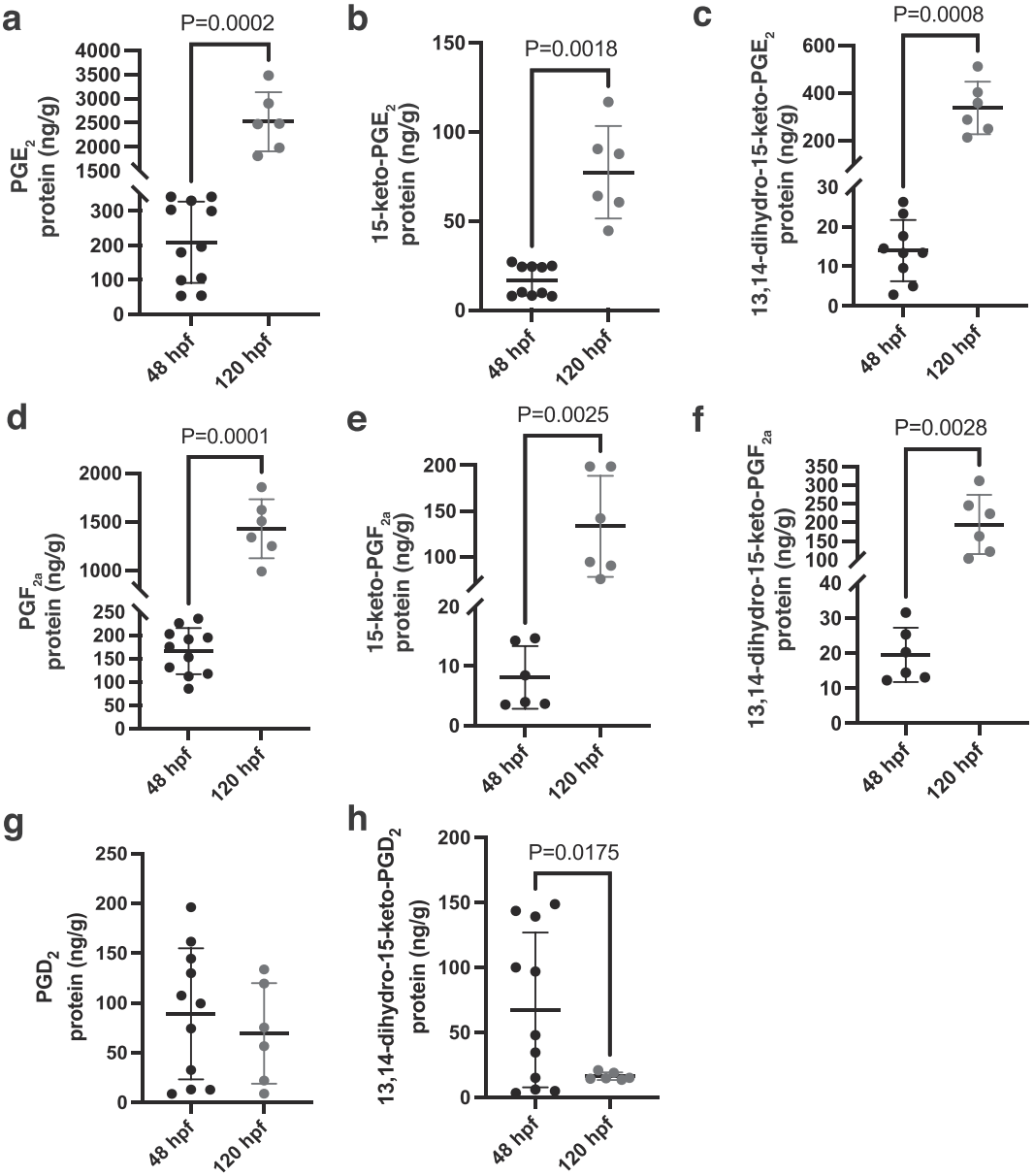

Fig. 2. Prostaglandin lipidomic profiles of developing zebrafish embryos. (a-h) Lipidomic analysis of whole zebrafish embryos at two different developmental stages (48 hpf and 120 hpf) showing the levels of the main prostaglandins and their metabolites: (a) PGE_2 ($P = 0.0002$), (b) 15-keto-PGE_2 ($P = 0.0018$), (c) 13,14-dihydro-15-keto-PGE_2 ($P = 0.0008$), (d) PGF_{2a} ($P = 0.0001$), (e) 15-keto-PGF_{2a} ($P = 0.0025$), (f) 13,14-dihydro-15-keto-PGF_{2a} ($P = 0.0028$), (g) PGD_2 ($P = 0.5006$) and (h) 13,14-dihydro-15-keto-PGD_2 ($P = 0.0175$). For 48 hpf: $N = 11$, $n = 275$ (less points in some of the graphs indicate missing values due to non-detectable levels). For 120 hpf: $N = 6$, $n = 150$. For all graphs, two-tailed unpaired *t*-test with Welch's correction was performed. Values are plotted as mean ± SD; $P < 0.05$ considered significant.

ligand stimulation (Fig. 1b). We incubated the transformed yeast cells with 100 nM PGE_2 or 1 μM 15-keto-PGE_2 for 20 min (Fig. 1c, d). For both hEP2 and hEP4, receptor count on the membrane was significantly increased after the stimulation with PGE_2 as well as with 15-keto-PGE_2 as compared to non-stimulated (absence of ligand) control condition (Fig. 1c, d). These observations suggest that apart from the well-established role of PGE_2 in activation of both EP2 and EP4 receptors [28,30,41–44], 15-keto-PGE_2 has also a potential of binding both EP2 and EP4 receptors and is able to stabilize their membrane localization.

In summary, our *in vitro* experiments indicate 15-keto-PGE_2 is able to bind both EP2 and EP4 receptors in agreement with other data [36]. Although 15-keto-PGE_2 has been shown to activate the production of cAMP *via* EP receptors [35], its downstream steps of receptor activation and signaling require further biochemical investigations. Whether 15-keto-PGE_2 has the bioactive potential to modulate the EP signaling *in vivo* needs to be elucidated.

2.2. PGE_2 is the most abundant prostaglandin during zebrafish embryonic development

To investigate the physiological role of 15-keto-PGE_2 *in vivo*, we used the zebrafish model having several advantageous attributes when it comes to testing the biological effects of small molecules and metabolites. First, we set out to determine what were the levels of 15-keto-PGE_2 in developing zebrafish embryos using the whole embryo lipidomic analysis. It is important to note that throughout the first developmental stages, *i.e.* until around 120 hpf, zebrafish embryo's nutrition depends on the yolk content [45]. Due to this dependency, metabolites and nutrients are not affected by exogenous factors like food intake, rendering the whole embryo lipidomic analysis reliable and fairly accurate [46].

We used the non-targeted metabolomic method based on liquid chromatography electrospray ionization tandem mass spectrometry (LC/ESI-MS/MS) to analyze the total prostaglandin metabolic pathway in the zebrafish embryos at two time points: 48 and 120 hpf, prior to and after the GFB formation, respectively (Fig. 2a-h). We determined the presence of all main prostaglandins, namely PGE_2, PGF_{2a} and PGD_2 as well as their catabolic products in the wild-type zebrafish whole embryo extracts (Fig. 2a-h). PGE_2 appeared to be the most abundant prostaglandin in both developmental stages (Fig. 2a). Markedly, the mean levels of PGE_2 and PGF_{2a} at 120 hpf (2522.13 ng/g and 1427.59 ng/g, respectively) were approximately by one order of magnitude higher compared to 48 hpf (209.36 ng/g and 165.98 ng/g, respectively) (Fig. 2a, d), while the levels of PGD_2 remained constant (Fig. 2g). Compared to PGE_2, its metabolite 15-keto-PGE_2 was also present but at approximately 10-fold lower levels than PGE_2, with the mean levels of 16.82 ng/g and 77.37 ng/g at 48 hpf and 120 hpf, respectively (Fig. 2b). 15-keto-PGE_2 showed higher levels compared to 15-keto-PGF_{2a} metabolite at 48 hpf, while both metabolites were present at similar levels at 120 hpf (Fig. 2b, e). The downstream metabolites of 15-keto-PG, *i.e.* 13,14-dihydro-15-keto-PG followed similar pattern (Fig. 2c, f, h).

Our data provide the quantitative analysis of the prostaglandin pathway during zebrafish development. We showed PGE_2 is the main prostaglandin present in the zebrafish embryos consistent with other animal models and humans [47–50]. Its metabolite, 15-keto-PGE_2 is also relatively highly abundant underscoring its potential role in organismal physiology.

2.3. 15-keto-PGE_2 exposure results in kidney morphological changes

Since PGE_2 has been reported to regulate the kidney development in zebrafish [44,51–53], we opted for investigating the potential biological role of 15-keto-PGE_2 in the kidney formation in this model. We followed a pharmacological approach similar to drug screenings that have previously established prostaglandin effects in the kidney morphogenesis [44]. Embryos were exposed to the DMSO vehicle and 15-keto-PGE_2 (500 μM) prior to the formation of GFB, from 6 hpf to 48 hpf (Fig. 3a).

We used the transgenic line *Tg[wt1b:eGFP]*, in which the parietal epithelium and podocytes of the glomeruli are labeled with GFP fluorescence, to perform phenotypic assessment of the embryo development as well as kidney formation by the combination of brightfield and fluorescence microscopy (Fig. 3b). Apart from the mild fluid accumulation (edema) observed in the yolk area at 48 hpf, no other major phenotypic defects were detected in the embryos after early treatment with 15-keto-PGE_2 (Fig. 3b). Importantly, cardiac development and function including blood circulation did not show any impairment, suggesting no major changes in the overall hemodynamics. However, the pronephros morphology was significantly affected and associated with the impaired glomerular development and defects in the pronephric tubules angle (Fig. 3b, c).

The observed defects in the kidney morphogenesis after 15-keto-PGE_2 exposure suggest, this metabolite may play a potential role in kidney biology. Of note, other organs including liver may be affected as

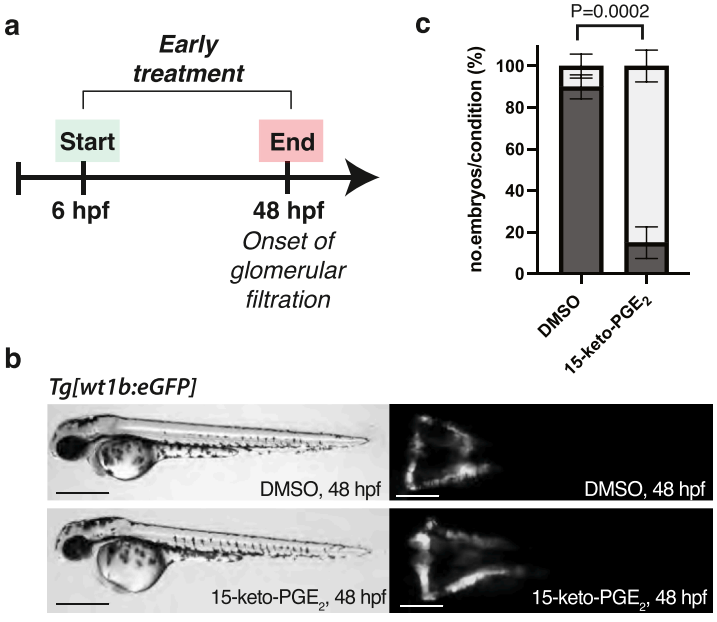

Fig. 3. Zebrafish pronephros is affected after early treatment with 15-keto-PGE_2. (a) Experimental design of the early pharmacological treatment, starting from 6 hpf until 48 hpf. (b) Brightfield and fluorescence microscopy images of *Tg[wt1b:eGFP]* embryos at 48 hpf, following pharmacological treatments with DMSO vehicle 0.88 % (upper panel) and 15-keto-PGE_2 500 μM (lower panel). Scale bar: 500 μm for brightfield images and 200 μm for fluorescent images. (c) Phenotypic quantitative analysis of zebrafish embryos at 48 hpf. Embryos are categorized as "no phenotype" (pronephros morphology remains unaffected after DMSO treatment) or "affected pronephros + yolk edema" (kidney phenotype observed after exposure to 15-keto-PGE_2); $N = 3$, $n = 30$ for both conditions; Percentage values are plotted as mean ± SD; n represents biologically independent samples over N independent experiments; Ordinary two-way ANOVA with Tukey's multiple comparison test ($P = 0.0002$); $P < 0.05$ considered significant.

well, but were not focus of this study.

2.4. Development and vascularization of glomerulus in the zebrafish embryonic kidney

To better understand the morphological changes in the glomerulus after the 15-keto-PGE_2 exposure, we decided to resolve the glomerular cytoarchitecture at the subcellular resolution using 3D confocal laser scanning microscopy. Glomerular morphology alters to a great extent during early kidney development, but its detailed visualization in the developing zebrafish is sparse [14,54–58]. We therefore first analyzed the critical steps in glomerular formation in *Tg[wt1b:EGFP]* in more detail (Fig. 4). In addition to the labeled podocytes and parietal epithelial cells in these transgenics, we performed the angiography using bovine serum albumin (BSA) conjugated with AlexaFluor555 to mark the endothelial cells of glomerular capillaries as previously described [59]. We visualized glomeruli development and its vascularization throughout five different stages; at 30, 48, 52, 72, 120 hpf. At 30 hpf, in nephron primordia stage (the most immature stage of the nephrons) the glomeruli appear as an unvascularized group of cells directly abutting the dorsal aorta in the midline of the embryo (Fig. 4, 30 hpf). At 48 hpf, endothelial cells start invading the space between the bilateral nephron primordia, forcing the invagination of the podocytes resulting in the formation of the glomerular cleft (Fig. 4, 48 hpf). A few hours later, at 52 hpf, the progressive invasion of endothelial cells drives the elaborated intercalation of podocytes around the continuously growing glomerular capillaries (Fig. 4, 52 hpf). At 72 hpf, the podocytes form finger-like projections interwoven with forming capillaries (Fig. 4, 72 hpf), resembling interlaced fingers of clasped hands. At this stage the formation of GFB is complete in zebrafish [14]. Between 72 and 120 hpf, the process of the complex infoldings between the endothelial cells and podocytes continues (Fig. 4, 120 hpf). Ultimately, the progressive infoldings of the GBM driven by cell-cell interactions between endothelial cells and podocytes lead to the complete maturation of the glomeruli along with the functional filtration apparatus.

Our detailed morphological analysis suggests the formation and the maturation of the GFB follow distinct steps that depend on the intricate cell-cell interaction between podocytes and endothelial cells throughout the entire process.

2.5. 15-keto-PGE_2 perturbs the proper GFB formation and maturation in zebrafish

The increased fluid flow shear stress in the glomeruli that arises for instance after unilateral nephrectomy [60], may result in elevated levels of PGE_2 linked to the podocyte damage and potential albuminuria [61,62]. Interestingly, the increased levels of PGE_2 and 15-keto-PGE_2 were also measured in a well-established Münich Wistar Frömter (MWF) rat model of CKD with glomerular hyperfiltration and albuminuria [30], but whether 15-keto-PGE_2 may contributes to the renal pathological phenotype is unresolved. Our results showing that the early treatment with 15-keto-PGE_2 led to possible alterations in glomerular structure (Fig. 3), prompted us to analyze the potential defects in glomerular cytoarchitecture using high-resolution confocal microscopy at the subcellular level (Fig. 5). The early treatment with 15-keto-PGE_2 caused defects in the invasion of endothelial cells as well as podocyte intercalation resulting in the absence of the proper glomerular cleft formation at 48 hpf (Fig. 5a, b). We were then curious whether any changes in glomerular cytoarchitecture could occur after the late treatment with 15-keto-PGE_2 from 72 hpf to 96 hpf, *i.e.* after the formation of GFB (Supplementary Fig. S1a, Fig. 5c, d). First, the late 15-keto-PGE_2 treatment resulted in the defects of the body axis, the absence of the swim bladder formation, and the expansion of the liver in the embryos at 96 hpf (Supplementary Fig. S1a, b). In the glomerulus, the late exposure to the 15-keto-PGE_2 metabolite had a profound impact on its maturation causing similar effects as after the early treatment; the podocyte intercalation around the glomerular capillaries was markedly impaired with the characteristic clustering of podocytes in the embryo midline (Fig. 5c, d).

Could these cellular defects result in the impairment of the GFB function? To that end, we used a GFP-tagged albumin surrogate (gc-EGFP) expressed in the transgenic line *Tg[fabp10a:gc-EGFP]* and circulating in the blood plasma [63]. This model has been widely used to evaluate the GFB integrity and function in zebrafish, since in the case of the GFB damage, the albumin surrogate leaks through the GFB, resulting in the loss of GFP fluorescence in the vasculature [53,63]. We did not observe any significant GFB permeability defects at 96 hpf as the GFP signal was comparable between the control and 15-keto-PGE_2-treated embryos (Supplementary Fig. S1b, c).

Our results demonstrate that 15-keto-PGE_2 can profoundly affect the interaction between podocytes and endothelial cells throughout the glomeruli formation, at the initial stage of glomerular cleft formation as well as during complex infoldings of the GBM, and suggest 15-keto-PGE_2 may have a potential active role in the fine-tuning of the GFB physiology. The fact that late treatment with 15-keto-PGE_2 did not affect GFB permeability may be due to several aspects including relatively short exposure time.

2.6. Glomerular surface area is significantly decreased after exogenous 15-keto-PGE_2 stimulation

To better understand how the impaired podocyte intercalation around the glomerular capillaries after 15-keto-PGE_2 treatment may affect GFB, we proceeded with further morphological analysis of the glomerulus. Using the Imaris software, we obtained the 3D glomerular reconstruction and surface creation by segmentation of the glomeruli labeled with GFP in *Tg[wt1b:eGFP]* transgenics at 96 hpf to quantify the glomerular volume and surface area in the DMSO-treated control and 15-keto-PGE_2-treated embryos (Fig. 6a-c). Glomerular volume showed a numerical decrease in the 15-keto-PGE_2-treated embryos as compared to DMSO controls (Fig. 6b). Importantly, the surface area covered by podocytes was significantly decreased after exposure to the 15-keto-PGE_2 metabolite (Fig. 6c).

The intercalation defects between podocytes and endothelial cells after 15-keto-PGE_2 exposure led to the reduction of GFB surface area that might ultimately affect the GFB function.

2.7. 15-keto-PGE_2-induced defects are mediated through EP2/EP4 receptors

We were wondering whether the 15-keto-PGE_2 treatment induced the observed morphological defects through EP receptor activation. Since our *in vitro* data indicated that 15-keto-PGE_2 binds both EP2 and EP4 receptors, we deployed EP antagonists, PF-04418948 and ONO-AE3-208, blocking EP2 and EP4, respectively. We simultaneously treated zebrafish embryos with 15-keto-PGE_2 and EP2 and EP4 antagonists to test whether blocking the receptors will dampen or block 15-keto-PGE_2-induced effects (Fig. 6a-c). Remarkably, the simultaneous pharmacological blockade of EP2 and EP4 receptors in 15-keto-PGE_2-treated embryos abolished the podocyte clustering and the complexity of the GBM infoldings was restored (Fig. 6a). The quantification of the glomerular volume as well as surface area revealed complete restoration of the 15-keto-PGE_2-induced effects when compared to the vehicle controls (Fig. 6b, c).

In summary, our data provide evidence for 15-keto-PGE_2 modulating EP2 and EP4 receptors signaling *in vivo*.

3. Discussion

The prostaglandin E_2 pathway plays a crucial role in various physiological and pathological conditions and has been extensively reported for its involvement in renal diseases [17,25–27,64,65]. However, the

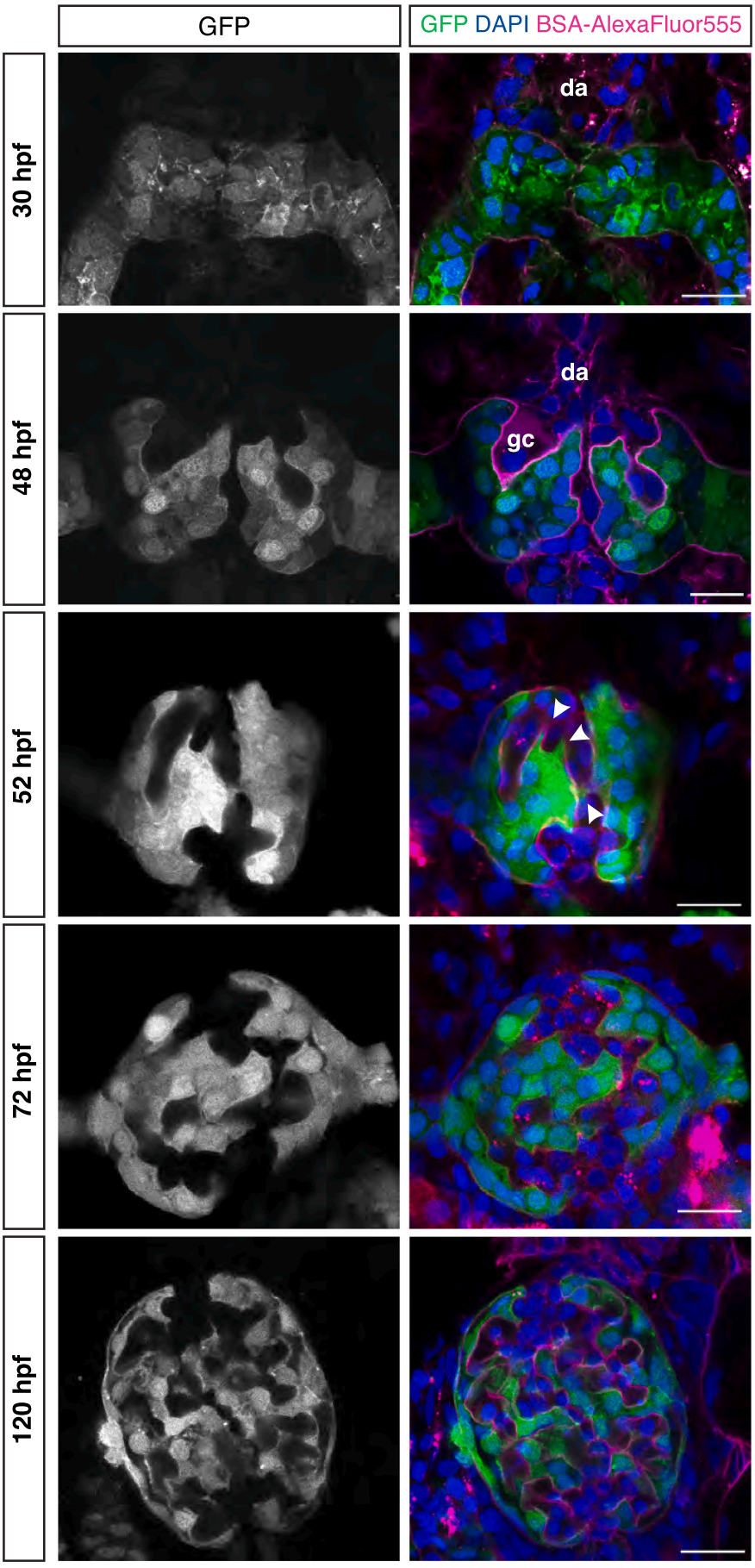

Fig. 4. Glomerular morphogenesis occurs in distinct steps. Zebrafish glomerular developmental stages. Representative high-resolution confocal microscopy images (single confocal section) of the *Tg[wt1b:eGFP]* developing zebrafish embryonic kidney at different developmental stages, 30 hpf (nephron primordia), 48 hpf, 52 hpf, 72 hpf and 120 hpf in an order from top to bottom. The podocytes and parietal epithelial cells in the glomeruli in grey (left), in green (in merge, right), endothelial cells of glomeruli capillaries in magenta (BSA-AlexaFluor555, in merge), cells nuclei in blue (DAPI, in merge). At 52 hpf, podocyte protrusions (arrowheads) start surrounding the capillaries to form the mature GFB. Dorsal aorta (da) and glomerular cleft (gc) are observed at the early developmental stages of the glomerulus. Scale bar = 10 μm. (For interpretation of the references to colour in this figure legend, the reader is referred to the web version of this article.)

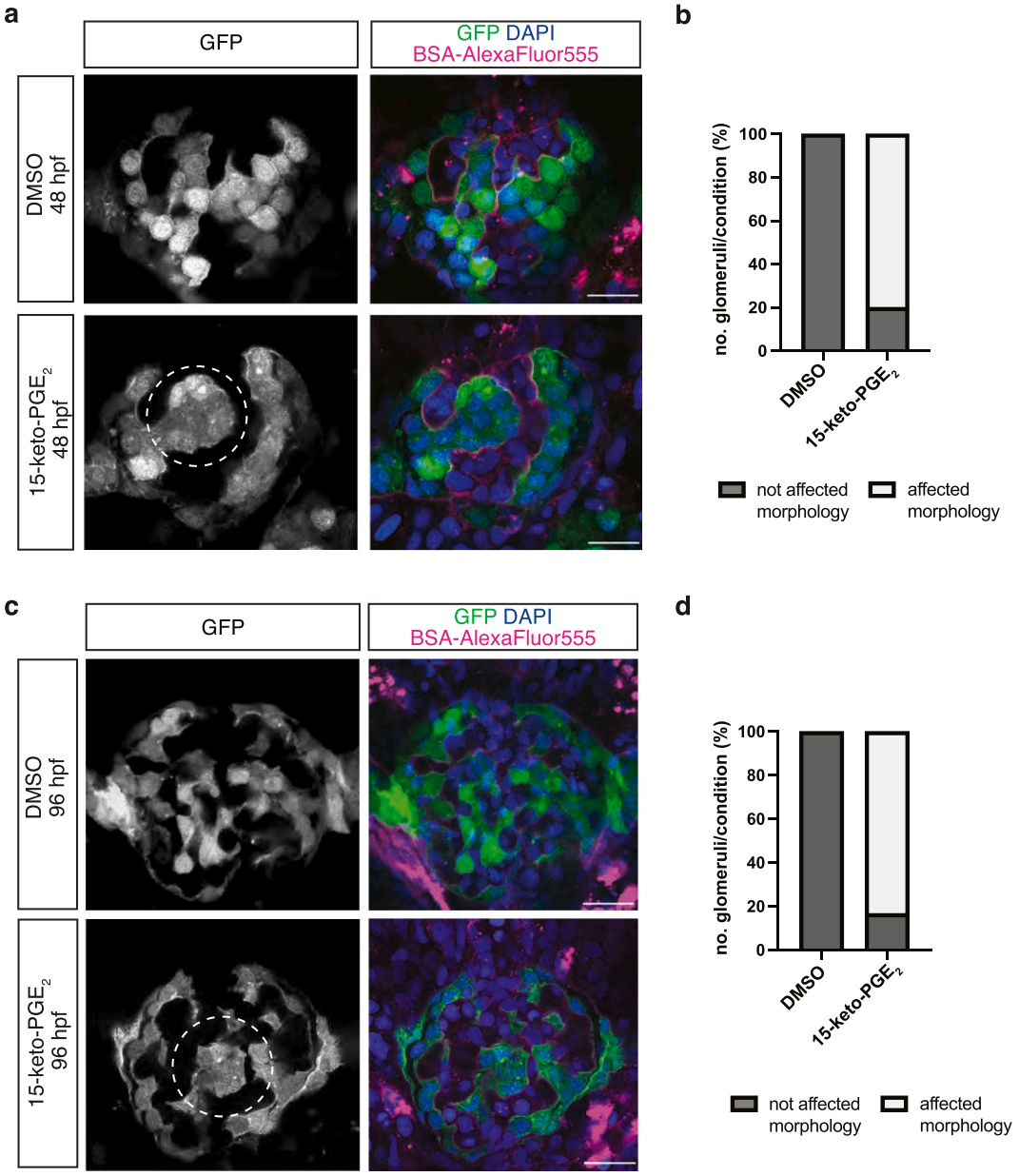

Fig. 5. 15-keto-PGE_2 exposure affects podocyte intercalation process during glomerular vascularization. (a) Representative confocal microscopy images of *Tg[wt1b:eGFP]* zebrafish glomeruli at 48 hpf after DMSO vehicle 0.88 % and 15-keto-PGE_2 500 μM treatment; $N = 2$, $n = 5$ for both conditions; dotted-line circle indicates podocyte consolidation and failure of normal elaboration around the continuously forming glomerular capillaries. (b) Quantification graph showing the percentage of imaged glomeruli with affected morphology at 48 hpf after exposure to DMSO (not affected morphology) and 15-keto-PGE_2 (4 out of 5 imaged glomeruli showed affected morphology). (c) Representative confocal microscopy images of *Tg[wt1b:eGFP]* zebrafish glomeruli at 96 hpf after DMSO vehicle 0.88 % and 15-keto-PGE_2 500 μM treatment; $N = 3$, $n = 7$ for DMSO and $N = 3$, $n = 6$ for 15-keto-PGE_2; dotted-line circle indicates impaired podocyte intercalation around the formed capillaries. (d) Quantification graph showing the percentage of imaged glomeruli with affected morphology at 96 hpf after exposure to DMSO (not affected morphology) and 15-keto-PGE_2 (5 out of 6 imaged glomeruli showed affected morphology). In all images, grey scale images show the podocytes and parietal epithelial cells in the glomeruli; in the merge podocytes and parietal epithelial cells are represented in green (eGFP), endothelial cells of glomeruli capillaries are marked in magenta (BSA-AlexaFluor555) and cells nuclei in blue (DAPI); Scale bar = 10 μm. (For interpretation of the references to colour in this figure legend, the reader is referred to the web version of this article.)

metabolic products of PGE_2 degradation, 15-keto-PGE_2 and 13,14-dihydro-15-keto-PGE_2, have been mainly considered biologically inactive [32,34]. Here, we show that 15-keto-PGE_2 affects the glomerular morphology of the developing zebrafish embryonic kidney through EP2/EP4 receptors. To our best knowledge, our study determines previously unrecognized *in vivo* effects of 15-keto-PGE_2 in kidney biology and outlines its possible modulatory effects on EP2/EP4 signaling.

In recent years, the potential bioactive role of 15-keto-PGE_2 has attracted increased research focus [37–39,66,67]. The 15-keto-PGE_2 effects have been mainly investigated in the context of the peroxisome proliferator-activated receptor gamma (PPAR-γ) signaling [37–39]. Through PPAR-γ activation, 15-keto-PGE_2 inhibits the production of lipopolysaccharide (LPS)-induced inflammatory cytokines in Kupffer cells [38], while in a zebrafish model of cryptococcosis, 15-keto-PGE_2 promotes fungal pathogenesis [37]. Another study demonstrated 15-keto-PGE_2 role in the activation of Nrf2/ARE (nuclear erythroid 2-related factor 2/antioxidant response element) pathway in macrophages in mice with experimental sepsis [66]. In addition, 15-keto-PGE_2

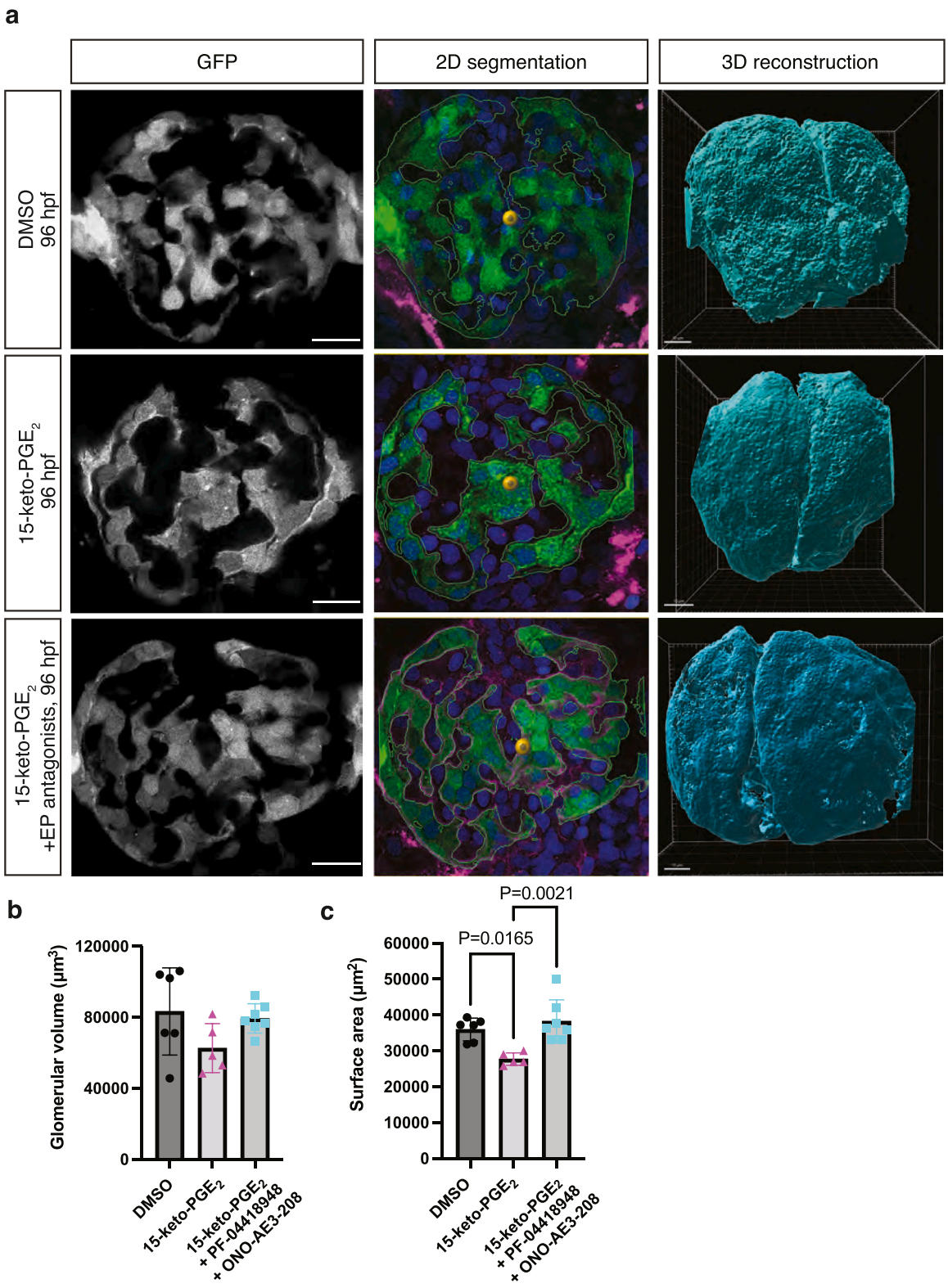

Fig. 6. Combined pharmacological blockade of EP2 and EP4 receptors reverses the effect of 15-keto-PGE_2 exposure. (a) Representative images of 2D surface segmentation and 3D glomerular reconstruction performed with Imaris software using the confocal microscopy images of *Tg[wt1b:eGFP]* zebrafish glomeruli at 96 hpf after pharmacological treatment with DMSO vehicle 0.96 % (top) ($N = 3$, $n = 6$), 15-keto-PGE_2 500 μM (middle) ($N = 3$, $n = 5$), and 15-keto-PGE_2 500 μM + PF-04418948 (EP2 receptor antagonist) 20 μM + ONO-AE3-208 (EP4 receptor antagonist) 20 μM (bottom) ($N = 2$, $n = 7$); *n* represents biologically independent samples over *N* independent experiments; Scale bar = 10 μm. (b-c) Quantitative graphs of the glomerular volume and surface area in the glomeruli analyzed for the different pharmacological treatment groups; Ordinary one-way ANOVA with Tukey's multiple comparison test was performed for both graphs; in graph (b): DMSO *vs* 15-keto-PGE_2 ($P = 0.1362$), 15-keto-PGE_2 *vs* 15-keto-PGE_2 + PF-04418948 + ONO-AE3-208 ($P = 0.2331$), and DMSO *vs* 15-keto-PGE_2 + PF-04418948 + ONO-AE3-208 ($P = 0.9074$); in graph (c): DMSO *vs* 15-keto-PGE_2 ($P = 0.0165$), 15-keto-PGE_2 *vs* 15-keto-PGE_2 + PF-04418948 + ONO-AE3-208 ($P = 0.0021$), and DMSO *vs* 15-keto-PGE_2 + PF-04418948 + ONO-AE3-208 ($P = 0.6048$); Values are plotted as mean ± SD; $P < 0.05$ considered significant.

has been also associated with different types of cancer, as it reportedly increases p21 promoter activity in hepatocellular carcinoma cells through PPAR-γ activation [39] and inhibits STAT3 signaling thus suppressing breast cancer progression in MCF10A-*ras* cells [67].

The importance of 15-keto-PGE_2 in the physiology and/or pathophysiology of the kidney has not been previously investigated. Nevertheless, the role of 15-hydroprostaglandin dehydrogenase (15-PGDH), the enzyme that catalyzes the first step of PGE_2 inactivation and synthesizes 15-keto-PGE_2, has been widely studied for its implication in kidney diseases. 15-PGDH inhibition prevents contrast-induced acute kidney injury [68], ischemic acute kidney injury (AKI) [69] and acute liposaccharide (LPS)-induced renal injury in mice [70]. In addition, 15-PGDH activity has been reported in rabbit kidney cortex [71,72] as well as in maternal rat kidney and fetal rat and lamb kidney [73]. All this evidence suggests that 15-keto-PGE_2 might have a potentially detrimental role in kidney biology.

In the present study, we show that 15-keto-PGE_2 stimulation *in vivo* affects glomerular morphology characterized by the podocyte intercalation defects around the glomerular capillaries in zebrafish embryos. The exogenous treatment with the metabolite does not considerably affect the glomerular volume, but results in the significant decrease of the glomerular surface area highlighting the impaired podocyte intercalation and reduced area of the glomerular filtration barrier. Combined pharmacological blockade of EP2 and EP4 receptors leads to complete reversal of the podocyte intercalation defects caused by 15-keto-PGE_2 exposure. This provides evidence for the role of 15-keto-PGE_2 in modulating EP2 and EP4 receptor signaling and is in agreement with a previous study supporting 15-keto-PGE_2 bioactive signaling *via* these receptors *in vitro* [36].

Our findings suggest a novel physiological role of 15-keto-PGE_2 in the proper GFB and glomerular surface area formation. Moreover, a potential role of this metabolite, in addition to PGE_2, in renal hemodynamics maintenance and blood pressure regulation should be taken into consideration. Given that we have recently shown 15-keto-PGE_2 levels are elevated in the isolated glomeruli of a well-established rat model of CKD with glomerular hyperfiltration and albuminuria [30], the question whether 15-keto-PGE_2 has potential pathophysiological effects in the context of renal biology should be addressed in the future studies. In addition, 15-keto-PGE_2 may affect renal vasculature that could be associated with glomerular hypertension and affect the proper podocyte intercalation, as observed here. Notwithstanding, the latter may outline the possible contribution of 15-keto-PGE_2 in the fine-tuning of the complex interactions between podocytes and endothelial cells that underlie glomerular vascularization and formation of functional and mature GFB.

PGE_2, described as a potent vasodilator in renal vasculature [74], has been widely studied in the regulation of renal hemodynamics, arterial blood pressure and renal blood flow [75–77]. In this context, EP2 and EP3 were highlighted to exert a crucial role in the PGE_2-induced renal hemodynamic responses and vascular functions [78,79]. To the best of our knowledge, implication of 15-keto-PGE_2 in renal hemodynamics is not yet known. Although, we cannot exclude of the potential regulatory effects of 15-keto-PGE_2 on renal hemodynamics, the fact that we do not observe any cardiac defects (the heart formation as well as function are not altered) suggests that overall hemodynamics seems to be unaffected. Second, we observe the defects in podocyte-endothelial interactions already early at the onset of glomerular filtration, *i.e.* before the fully functional glomerular filtration occur, pointing more towards the direct cell-cell interaction deregulation rather than through the hemodynamics alterations. However, to clarify this, further investigation including renal blood flow measurements to assess a potential vasoconstrictor or vasodilator effect of 15-keto-PGE_2, is required.

Altogether, our findings reveal 15-keto-PGE_2 metabolite may modulate EP2 and EP4-dependent signaling during glomerular morphogenesis. Whether this involves full receptor activation or whether 15-keto-PGE_2 acts in dominant negative manner or whether its effects are indirect needs to be further elucidated. Whether in pathological conditions elevated levels of 15-keto-PGE_2 might change podocyte-endothelial cell interactions warrant further studies.

4. Methods

4.1. Zebrafish husbandry

Zebrafish (*Danio rerio*) were bred, raised, and maintained in accordance with the FELASA guidelines [80], the guidelines of the Max-Delbrück Center for Molecular Medicine in the Helmholtz association and the local authority for animal protection (Landesamt für Gesundheit und Soziales, Berlin, Germany). The 'Principles of Laboratory Animal Care' (NIH publication no. 86–23, revised 1985) as well as the current version of German Law on the Protection of Animals and EU directive 2010/63/EU on the protection of animals were followed. Zebrafish transgenic lines used in this study included *Tg(wt1b:eGFP)*^{li1} [81] and *Tg(fabp:gc-EGFP)*^{mi1000} [63]. Embryos were kept in E3 embryo medium (5 mM NaCl, 0.17 mM KCl, 0.33 mM $CaCl_2$, 0.33 mM $MgSO_4$, pH 7.4) under standard laboratory conditions at 28.5 °C in all the experiments.

4.2. Generation of HiBiT-tagged hEP2/hEP4 receptor constructs

To generate hEP2−/hEP4-HiBiT constructs with a HiBiT-taq, the full-length human Prostaglandin E Receptor 2 (hEP2) and human Prostaglandin E Receptor 4 (hEP4) cDNAs were cloned into the pBiT3.1-N [CMV/HiBiT/Blast] vector (Promega) including a short linker attached to the N-terminal receptor sequences. Briefly, template cDNA was prepared from conditionally immortalized human podocytes [82]. Cloning primers were designed spanning either the start codon (forward-primers) or stop codon (reverse-primers) of the hEP2/hEP4 receptor sequences and having 5′ end extensions complementary to the linearized pBiT3.1-N [CMV/HiBiT/Blast] vector containing a restriction site. Primer sequences are listed in Table 1. Full-length hEP2 and hEP4 cDNA sequences were amplified using CloneAmp HiFi PCR Premix (TaKaRa Bio Inc.) and the designed cloning primers.

Restriction digestion of the pBiT3.1-N [CMV/HiBiT/Blast] vector was performed using CutSmart™ Buffer (New England Biolabs) and *EcoR*I and *Xba*I restriction enzymes (New England Biolabs). The PCR products were integrated into the vector using the 5X In-Fusion® HD Enzyme Premix (TaKaRa Bio Inc.) and the resulting plasmid was transformed into One Shot™ TOP10 chemically competent *E.coli* (Thermo Fisher Scientific). The plasmid sequences were verified by Sanger sequencing (LGC genomics).

For transformation into yeast, the hEP2-/hEP4-HiBiT constructs were cloned into the p426GPD yeast plasmid (GlxoSmithKline) [40] using cloning primers listed in Table 1. The forward primer with a 5′ overhang complementary to the yeast plasmid, spanning a *BamH*I restriction site and the HiBiT-tag start codon was designed. The reverse primers with a 5'overhang spanning a restriction site close to the stop codon of the hEP2/hEP4 sequence as well as the respective stop codon were designed. Purified pBiT3.1-N [CMV/HiBiT/Blast] vector (Promega) with integrated hEP2/hEP4 sequence was used as a template for PCR amplification using CloneAmp HiFi PCR Premix (TaKaRa Bio Inc.). Linearized plasmids and PCR products were purified and integrated into the p426GPD, ligation of the plasmid was conducted with the 5X In-Fusion® HD Enzyme Premix (TaKaRa Bio Inc.), the plasmids were transformed into One Shot™ TOP10 chemically competent *E.coli* (Thermo Fisher Scientific). The plasmid sequences were verified by Sanger sequencing (LGC genomics).

4.3. Yeast transformation

P426GPD plasmids carrying either hEP2-HiBiT or hEP4-HiBiT construct were transformed into *S.cerevisiae* (MMY yeast model, GlaxcoSmithKline) using lithium acetate (LiAc)/single-stranded DNA

Table 1
Primer sequences.

Construct name	Forward Primer (5′-3′)	Reverse Primer (5′-3′)
hEP2-HiBiT	CGAGCGGTGGGAATTCGATGGGCAATGCCTCCAATGAC	AAGCTTGACCTCTAGATCAAAGGTCAGCCTGTTTACTGGC
hEP4-HiBiT	CGAGCGGTGGGAATTCCATGTCCACTCCCGGGGTC	AAGCTTGACCTCTAGATTATATACATTTTTCTGATAAGTTCAGTGTTTCACT
hEP2-HiBiT-p426GDP	TAGAACTAGTGGATCCATGGTGAGCGGCTGGCGG	GCTTGATATCGAATTCTCAAAGGTCAGCCTGTTTACTGGC
hEP4-HiBiT-p426GDP	TAGAACTAGTGGATCCATGGTGAGCGGCTGGCGG	GCTTGATATCGAATTCTTATATACATTTTTCTGATAAGTTC

(ssDNA)/polyethylene glycol (PEG) method as previously described [40]. Briefly, 100 mL of yeast extract peptone dextrose (YPD) medium was inoculated with 1.5 mL yeast pre-culture and incubated for 2 h shaking at 30°. Yeast cultures were centrifuged at 600*g* for 2 min, washed with water, centrifuged at 600*g* for 1 min and the yeast pellets were suspended in 1 mL LiAcTE. For transformation, 5 μL of ssDNA (10 mg/mL, Sigma-Aldrich), 1 μg plasmids and for mock-transformed controls the corresponding volume of Midiprep Tris buffer solution (Macherey-Nagel), 50 μL yeast solution and 300 μL LiAc PEG TE were mixed by pipetting. After incubation at room temperature for 10 min and heat shock at 42 °C for 20 min, yeast solutions were plated on WHAUL plates supplemented with histidine (WHAUL-His).

4.4. Yeast strain and yeast culture

The used MMY28 yeast strain [40] has the following genotype: *W303-1A fus1::FUS1-HIS3 FUS1-lacZ::LEU2 far1Δ::ura3Δ gpa1Δ::ADE2Δ sst2Δ::ura3Δ MMY9 ste2Δ::G418^R TRP1::Gpa1/G$_{as(5)}$*. Prior to transformation, yeasts stored on glycerol beads at −80 °C were thawed and plated on YPD plates for 2 days at 30 °C before liquid pre-cultures were incubated in YPD medium shaking overnight at 30 °C. Transformed yeasts grew on WHAUL-His plates for three days. Three clones were picked and transferred on new WHAUL-His plates and incubated overnight at 30 °C. On the next day, prior to the experiments, clones were pre-cultured in WHAUL-His medium overnight shaking at 30 °C in flat 96-well plates (TPP).

4.5. Receptor expression on the yeast cell surface

The expressions of hEP2 receptor and hEP4 receptor on the yeast membrane were investigated with the NanoGlo® Extracellular Detection System (Promega Corporation). The system's principle is based on the expression of a HiBiT-tagged protein/receptor, which upon the incubation with the NanoGlo® Extracellular reagent produces a luminometry signal that reflects the number of receptors on the plasma membrane. If the added ligand of interest is able to bind the HiBiT-tagged receptor, it triggers a modification in the receptor's expression on the plasma membrane, which is manifested by a change in the luminometry signal.

Yeast pre-cultures were diluted 1:5 in WHAUL-medium and 5 μL of yeast dilution were incubated with 100 μL WHAUL-medium supplemented with BU Salts for 20 h. Following 20 h incubation, yeasts were stimulated for 20 min with 100 nM PGE_2, 1 μM 15-keto-PGE_2 or medium only for untreated control. Nine transformed colonies as well as one mock-transformed colony that served as a negative control were investigated at a time. Then, yeasts were treated with the Nano-Glo® Extracellular Detection System according to the manufacturer's instructions. Briefly, yeast solutions after stimulation were transferred to white 96-well plates (Corning Inc.). Thereby, one stimulated yeast solution was split into 2 wells after mixing. Equal volume of the reagent (consisting of NanoGlo® Extracellular Detection Buffer, NanoGlo® HiBiT Extracellular Substrate diluted 1:50 and LgBiT Protein diluted 1:100) was added to the yeast solutions. After 5 min shaking at 300 rpm for 5 min, luminescence was determined with the FLUOstar Omega microplate reader (BMG Labtech) and results were obtained using the Optima software and MARS data analysis software (BMG Labtech). Yeasts with luminescence lower than values of the medium control and the negative (mock-transformed) yeast control were excluded from the analysis, as the transformation was considered unsuccessful.

4.6. Lipidomic analysis of the whole zebrafish embryos

The lipidomic analysis was performed by liquid chromatography electrospray ionization tandem mass spectrometry (LC/ESI-MS/MS) following the protocol we reported recently [30]. The zebrafish embryos at two different developmental stages, 48 hpf and 120 hpf, were frozen using liquid nitrogen and analyzed using an Agilent 1290 HPLC system with binary pump, multisampler and column thermostat with a Zorbax Eclipse plus C-18, 2.1 × 150 mm, 1.8 μm column using a solvent system of aqueous acetic acid (0.05 %) and acetonitrile. A gradient starting with 5 % organic phase was used, which was increased within 0.5 min to 32 %, 16 min to 36.5 %, 20 min to 38 %, 28 min to 98 % and held there for 5 min, was used for the elution. The flow rate was set at 0.3 mL/min and the injection volume was 20 μL. The HPLC was coupled with an Agilent 6495 Triplequad mass spectrometer (Agilent Technologies, Santa Clara, CA, USA) with electrospray ionization source. Source parameters: Drying gas: 115 °C/16 L/min, Sheath gas: 390 °C/12 L/min, Capillary voltage: 4300 V, Nozzle voltage: 1950 V, and Nebulizer pressure: 35 psi.

4.7. Pharmacological treatment, glomerular morphology and functional assessment of the GFB

For the phenotypic assessment of the zebrafish embryonic kidney and the evaluation of GFB integrity the transgenic lines *Tg[wt1b:eGFP]* and *Tg[fabp10a:gc-eGFP*] were used, respectively. For the drug treatment, the E3 medium was completely drawn off the embryos and the solution of DMSO (% adjusted to the solvent ratio in drug solution) (276855, Sigma Aldrich), and 500 μM 15-keto-PGE_2 (Cay14720-1, Cayman) in E3 water were added. For the combined blockade of EP2 and EP4 receptors, a solution of 20 μM EP2 receptor antagonist (PF04418948, Sigma Aldrich) and 20 μM EP4 receptor antagonist (ONO-AE3-208, Sigma Aldrich) in E3 water with 500 μM 15-keto-PGE_2 was used. The drugs were applied to the zebrafish embryos between 6 hpf and 48 hpf for the early treatment and between 72 hpf and 96 hpf for the late treatment. The embryos were placed in a 28.5 °C incubator until phenotypic analysis. For the *in vivo* imaging, 48 hpf and 96 hpf zebrafish embryos were anesthetized with 0.02 % tricaine (*w/v*) in E3 solution and embedded in methyl cellulose. Fluorescent and brightfield images were acquired using Leica M165 stereomicroscope with a Leica DFC450 camera attached.

4.8. Confocal microscopy of zebrafish embryonic kidney and 3D reconstruction of the glomerulus

For the confocal imaging, *Tg[wt1b:eGFP]* zebrafish embryos were used at the time points indicated in the figure legend. Prior to the fixation, the anesthetized embryos (in 0.02 % tricaine (w/v)) were injected in the sinus venosus or the descending cardinal vein with 20 mg/mL BSA Alexa Fluor555 conjugate (A34786, ThermoFisher Scientific) diluted in in 150 mM NaCl. The injected embryos were fixed after 20 min in 4 % PFA (43369, Alfa Aesar) and 0.1 % Triton-X 100 in PBS buffer (D8357, Sigma Aldrich) for 2 h at RT or overnight at 4 °C. Nuclei were stained using 4′,6-Diamidin-2-phenylindol (DAPI, Sigma Aldrich, stock solution 1 mg/mL diluted 1:2000 in PBS) overnight at 4 °C. After removal of the

yolk and mounting in 0,8 % low-melting agarose, the kidneys of whole-mount fixed embryos were imaged using a Confocal Zeiss LSM 980 Airyscan microscope with a LD C-Apochromat 40 x NA1.1 water objective and Zen Blue v.3.2 software. Confocal z-stacks of all channels were sequentially acquired with identical parameters and similar 3D orientation for all samples. Images were analyzed using ImageJ software.

The 3D confocal images were first deconvolved using Huygens Professional 22.04 software. The 2D segmentation for the 3D glomerular surface creation, was performed using Imaris version 9.9 software (Bitplane AG, Zurich, Switzerland). A 3D surface covering the total glomerular volume was created by manually tracing the surface outline of EGFP-positive cells for every second section of the z-stack and in a second step the automated segmentation for the surface creation was used. The fluorescence signal derived by EGFP-positive cells inside the glomeruli was included, while EGFP signal coming from the neck and the early part of proximal convoluted tubule was excluded.

4.9. Statistical analysis

Statistics were performed using GraphPad Prism version 6.07 or 9. Following statistical tests were used: Fig. 1c,d, Wilcoxon test and Mann-Whitney tests were conducted as indicated (*, $P < 0.05$; **, $P < 0.01$; ***, $P < 0.001$; **** $P < 0.0001$); Fig. 2, two-tailed unpaired *t*-test with Welch's correction; Fig. 3c, two-way ANOVA with Tukey's multiple comparisons; Fig. 6b, c, one-way ANOVA with Tukey's multiple comparisons post-test. Identification of outliers was performed by Grubbs' outliers test ($\alpha = 0.05$). Excluded values: Fig. 1b, c: one outlier was identified among EP2-transfected and two outliers among EP4-transfected yeasts (for all yeast experiments conducted at the same day); Fig. 2: one outlier was identified and removed among the lipidomic PGE_2 values at 48 hpf together with the respective values for the two metabolites; Fig. 6b, c: one outlier was identified in the glomerulus surface area measurements each for the DMSO and 15-keto-PGE_2 condition that were excluded both from the surface area and also the glomerular volume analysis. In all graphs error bars are presented as means ± SD and $P < 0.05$ were considered statistically significant.

Supplementary data to this article can be found online at https://doi.org/10.1016/j.lfs.2022.121114.

CRediT authorship contribution statement

Conceptualization, A.K., J.B., R.K. and D.P.; Methodology and experimentation, A.K., D.K.G., A.P., R.C., A.S, E.M., A.Sch.; Data analysis, A.K., D.K.G, M.R.; Visualization, A.K., D.K.G. and D.P.; Writing – Original Draft, A.K. and D.P. with input from all authors; Revised manuscript, A.K. and D.P.; Funding Acquisition, R.K. and D.P.; Supervision, A.P., R.C., J.B., R.K. and D.P.

Declarations

All methods were carried out in accordance with relevant guidelines and regulations.

The study was carried out in compliance with the ARRIVE guidelines.

Declaration of competing interest

The authors declare that they have no known competing financial interests or personal relationships that could have appeared to influence the work reported in this paper.

Data availability

Data will be made available on request.

Acknowledgements

We thank Christoph Englert (Leibniz Institute on Ageing) and Weibin Zhou (University of Michigan) for sharing the fish *Tg(wt1b:eGFP)* and *Tg (fabp:gc-EGFP)* transgenic lines, respectively. We thank Moin A. Saleem (University of Bristol, UK) for sharing human podocytes line and Simon Dowell (GSK, Stevenage, United Kingdom) for providing the p426GPD yeast plasmid and the yeast strain. We thank Alexander M. Meyer for expert technical support, and the Aquatic Facility and Advanced Light Microscopy Technology Platform at MDC. Work for this project was supported by the Deutsche Forschungsgemeinschaft (DFG, German Research Foundation)—project number 394046635—SFB 1365.

References

[1] F. Costantini, R. Kopan, Patterning a complex organ: branching morphogenesis and nephron segmentation in kidney development, Dev. Cell 18 (2010) 698–712, https://doi.org/10.1016/j.devcel.2010.04.008.
[2] M. Krause, A. Rak-Raszewska, I. Pietilä, S. Quaggin, S. Vainio, Signaling during kidney development, Cells. 4 (2015) 112–132, https://doi.org/10.3390/cells4020112.
[3] W. Kriz, B. Kaissling, Structural organization of the mammalian kidney, in: Seldin and Giebisch's The Kidney, Elsevier, 2008, pp. 479–563, https://doi.org/10.1016/B978-012088488-9.50023-1.
[4] A.P. McMahon, Development of the Mammalian Kidney, 1st ed., Elsevier Inc., 2016 https://doi.org/10.1016/bs.ctdb.2015.10.010.
[5] K. Ebefors, E. Lassén, N. Anandakrishnan, E.U. Azeloglu, I.S. Daehn, Modeling the glomerular filtration barrier and intercellular crosstalk, Front. Physiol. 12 (2021), https://doi.org/10.3389/fphys.2021.689083.
[6] A. Pozzi, G. Jarad, G.W. Moeckel, S. Coffa, X. Zhang, L. Gewin, V. Eremina, B. G. Hudson, D.B. Borza, R.C. Harris, L.B. Holzman, C.L. Phillips, R. Fassler, S. E. Quaggin, J.H. Miner, R. Zent, B1 integrin expression by podocytes is required to maintain glomerular structural integrity, Dev. Biol. 316 (2008) 288–301, https://doi.org/10.1016/j.ydbio.2008.01.022.
[7] B. Haraldsson, J. Nyström, W.M. Deen, Properties of the glomerular barrier and mechanisms of proteinuria, Physiol. Rev. 88 (2008) 451–487, https://doi.org/10.1152/physrev.00055.2006.
[8] L. Butt, D. Unnersjö-Jess, M. Höhne, A. Edwards, J. Binz-Lotter, D. Reilly, R. Hahnfeldt, V. Ziegler, K. Fremter, M.M. Rinschen, M. Helmstädter, L.K. Ebert, H. Castrop, M.J. Hackl, G. Walz, P.T. Brinkkoetter, M.C. Liebau, K. Tory, P. F. Hoyer, B.B. Beck, H. Brismar, H. Blom, B. Schermer, T. Benzing, A molecular mechanism explaining albuminuria in kidney disease, Nat. Metab. 2 (2020) 461–474, https://doi.org/10.1038/s42255-020-0204-y.
[9] R.A. Wingert, A.J. Davidson, The zebrafish pronephros: a model to study nephron segmentation, Kidney Int. 73 (2008) 1120–1127, https://doi.org/10.1038/ki.2008.37.
[10] M. Elmonem, S. Berlingerio, L. van den Heuvel, P. de Witte, M. Lowe, E. Levtchenko, Genetic renal diseases: the emerging role of zebrafish models, Cells. 7 (2018) 130, https://doi.org/10.3390/cells7090130.
[11] G.F. Gerlach, R.A. Wingert, Kidney organogenesis in the zebrafish: insights into vertebrate nephrogenesis and regeneration, Wiley Interdiscip. RevDev. Biol. 2 (2013) 559–585, https://doi.org/10.1002/wdev.92.
[12] C. Santoriello, L.I. Zon, Hooked! Modeling human disease in zebrafish, J. Clin. Invest. 122 (2012) 2337–2343, https://doi.org/10.1172/JCI60434.
[13] P. Outtandy, C. Russell, R. Kleta, D. Bockenhauer, Zebrafish as a model for kidney function and disease, Pediatr. Nephrol. 34 (2019) 751–762, https://doi.org/10.1007/s00467-018-3921-7.
[14] I.A. Drummond, A.J. Davidson, Zebrafish kidney development, Methods Cell Biol. (2016), https://doi.org/10.1016/bs.mcb.2016.03.041.
[15] A.G. Kramer-Zucker, S. Wiessner, A.M. Jensen, I.A. Drummond, Organization of the pronephric filtration apparatus in zebrafish requires nephrin, podocin and the FERM domain protein mosaic eyes, Dev. Biol. 285 (2005) 316–329, https://doi.org/10.1016/j.ydbio.2005.06.038.
[16] J.Y. Park, M.H. Pillinger, S.B. Abramson, Prostaglandin E2 synthesis and secretion: the role of PGE2 synthases, Clin. Immunol. 119 (2006) 229–240, https://doi.org/10.1016/j.clim.2006.01.016.
[17] Y. Li, W. Xia, F. Zhao, Z. Wen, A. Zhang, S. Huang, Z. Jia, Y. Zhang, Prostaglandins in the pathogenesis of kidney diseases. www.oncotarget.com, 2018.
[18] K.C. Ugwuagbo, S. Maiti, A. Omar, S. Hunter, B. Nault, C. Northam, M. Majumder, Prostaglandin E2 promotes embryonic vascular development and maturation in zebrafish, Biol. Open. 8 (2019), https://doi.org/10.1242/bio.039768.
[19] T.E. North, W. Goessling, C.R. Walkley, C. Lengerke, K.R. Kopani, A.M. Lord, G. J. Weber, T.V. Bowman, I.H. Jang, T. Grosser, G.A. Fitzgerald, G.Q. Daley, S. H. Orkin, L.I. Zon, Prostaglandin E2 regulates vertebrate haematopoietic stem cell homeostasis, Nature 447 (2007) 1007–1011, https://doi.org/10.1038/nature05883.
[20] R. Iwasaki, K. Tsuge, K. Kishimoto, Y. Hayashi, T. Iwaana, H. Hohjoh, T. Inazumi, A. Kawahara, S. Tsuchiya, Y. Sugimoto, Essential role of prostaglandin E2 and the EP3 receptor in lymphatic vessel development during zebrafish embryogenesis, Sci. Rep. 9 (2019) 1–11, https://doi.org/10.1038/s41598-019-44095-5.
[21] W. Goessling, T.E. North, S. Loewer, A.M. Lord, S. Lee, C.L. Stoick-Cooper, G. Weidinger, M. Puder, G.Q. Daley, R.T. Moon, L.I. Zon, Genetic interaction of

PGE2 and wnt signaling regulates developmental specification of stem cells and regeneration, Cell 136 (2009) 1136–1147, https://doi.org/10.1016/j.cell.2009.01.015.
[22] S. Nissim, R.I. Sherwood, J. Wucherpfennig, D. Saunders, J.M. Harris, V. Esain, K. J. Carroll, G.M. Frechette, A.J. Kim, K.L. Hwang, C.C. Cutting, S. Elledge, T. E. North, W. Goessling, Prostaglandin E2 regulates liver versus pancreas cell-fate decisions and endodermal outgrowth, Dev. Cell 28 (2014) 423–437, https://doi.org/10.1016/j.devcel.2014.01.006.
[23] J. Hoggatt, P. Singh, J. Sampath, L.M. Pelus, Prostaglandin E2 enhances hematopoietic stem cell homing, survival, and proliferation, Blood 113 (2009) 5444–5455, https://doi.org/10.1182/blood-2009-01-201335.
[24] G. O'Callaghan, A. Houston, Prostaglandin E2 and the EP receptors in malignancy: possible therapeutic targets? Br. J. Pharmacol. 172 (2015) 5239–5250, https://doi.org/10.1111/bph.13331.
[25] V.L. Hood, Prostaglandins and the Kidney, 1977. http://ajprenal.physiology.org/.
[26] R. Nasrallah, R. Hassouneh, R.L. Hébert, PGE2, kidney disease, and cardiovascular risk: beyond hypertension and diabetes, J. Am. Soc. Nephrol. 27 (2016) 666–676, https://doi.org/10.1681/ASN.2015050528.
[27] R. Nasrallah, R. Hassouneh, R.L. Hébert, Chronic kidney disease: targeting prostaglandin E 2 receptors, Am. J. Physiol. Ren. Physiol. 307 (2014) 243–250, https://doi.org/10.1152/ajprenal.00224.2014.-Chronic.
[28] Y. Sugimoto, S. Narumiya, Prostaglandin E receptors, J. Biol. Chem. 282 (2007) 11613–11617, https://doi.org/10.1074/jbc.R600038200.
[29] L. Li, M.N. Sluter, Y. Yu, J. Jiang, Prostaglandin E receptors as targets for ischemic stroke: novel evidence and molecular mechanisms of efficacy, Pharmacol. Res. 163 (2021), 105238, https://doi.org/10.1016/j.phrs.2020.105238.
[30] E. Mangelsen, M. Rothe, A. Schulz, A. Kourpa, D. Panáková, R. Kreutz, J. Bolbrinker, Concerted EP2 and EP4 receptor signaling stimulates autocrine prostaglandin E2 activation in human podocytes, Cells. 9 (2020), https://doi.org/10.3390/cells9051256.
[31] R.J. Anderson, T. Berl, K.M. McDonald, R.W. Schrier, Prostaglandins: effects on blood pressure, renal blood flow, sodium and water excretion, Kidney Int. 10 (1976) 205–215, https://doi.org/10.1038/ki.1976.99.
[32] H.-H. Tai, C.M. Ensor, M. Tong, H. Zhou, F. Yan, Prostaglandin catabolizing enzymes, 2002.
[33] Y.H. Wu, T.P. Ko, R.T. Guo, S.M. Hu, L.M. Chuang, A.H.H.J. Wang, Structural basis for catalytic and inhibitory mechanisms of human prostaglandin reductase PTGR2, Structure (2008), https://doi.org/10.1016/j.str.2008.09.007.
[34] W.L. Chou, L.M. Chuang, C.C. Chou, A.H.J. Wang, J.A. Lawson, G.A. FitzGerald, Z. F. Chang, Identification of a novel prostaglandin reductase reveals the involvement of prostaglandin E2 catabolism in regulation of peroxisome proliferator-activated receptor γ activation, J. Biol. Chem. 282 (2007) 18162–18172, https://doi.org/10.1074/jbc.M702289200.
[35] N. Nishigaki, M. Negishi, A. Ichikawa, Two gs-coupled prostaglandin E receptor subtypes, EP2 and EP4, differ in desensitization and sensitivity to the metabolic inactivation of the agonist, Mol. Pharmacol. 50 (1996), 1031 LP – 1037, http://molpharm.aspetjournals.org/content/50/4/1031.abstract.
[36] S. Endo, A. Suganami, K. Fukushima, K. Senoo, Y. Araki, J.W. Regan, M. Mashimo, Y. Tamura, H. Fujino, 15-keto-PGE2 acts as a biased/partial agonist to terminate PGE2-evoked signaling, J. Biol. Chem. 295 (2020) 13338–13352, https://doi.org/10.1074/jbc.ra120.013988.
[37] R.J. Evans, K. Pline, C.A. Loynes, S. Needs, M. Aldrovandi, J. Tiefenbach, E. Bielska, R.E. Rubino, C.J. Nicol, R.C. May, H.M. Krause, V.B. O'Donnell, S. A. Renshaw, S.A. Johnston, 15-keto-prostaglandin e2 activates host peroxisome proliferator-activated receptor gamma (Ppar-γ) to promote cryptococcus neoformans growth during infection, PLoS Pathog. 15 (2019) 1–28, https://doi.org/10.1371/journal.ppat.1007597.
[38] L. Yao, W. Chen, K. Song, C. Han, C.R. Gandhi, K. Lim, T. Wu, 15-hydroxyprostaglandin dehydrogenase (15-PGDH) prevents lipopolysaccharide (LPS)-induced acute liver injury, PLoS One. 12 (2017) 1–16, https://doi.org/10.1371/journal.pone.0176106.
[39] D. Lu, C. Han, T. Wu, 15-PGDH inhibits hepatocellular carcinoma growth through 15-keto-PGE2/PPARγ-mediated activation of p21WAF1/Cip1, Oncogene 33 (2014) 1101–1112, https://doi.org/10.1038/onc.2013.69.
[40] S.J. Dowell, A.J. Brown, Yeast assays for G protein-coupled receptors, Methods Mol. Biol. 552 (2009) 213–229, https://doi.org/10.1007/978-1-60327-317-6_15.
[41] Y.I. Cha, S.H. Kim, D. Sepich, F. Gregory Buchanan, L. Solnica-Krezel, R.N. DuBois, Cyclooxygenase-1-derived PGE2 promotes cell motility via the G-protein-coupled EP4 receptor during vertebrate gastrulation, Genes Dev. 20 (2006) 77–86, https://doi.org/10.1101/gad.1374506.
[42] I. Dey, M. Lejeune, K. Chadee, Prostaglandin E 2 receptor distribution and function in the gastrointestinal tract, Br. J. Pharmacol. 149 (2006) 611–623, https://doi.org/10.1038/sj.bjp.0706923.
[43] H. Reinold, S. Ahmadi, U.B. Depner, B. Layh, C. Heindl, M. Hamza, A. Pahl, K. Brune, S. Narumiya, U. Müller, H.U. Zeilhofer, Spinal inflammatory hyperalgesia is mediated by prostaglandin E receptors of the EP2 subtype, J. Clin. Invest. 115 (2005) 673–679, https://doi.org/10.1172/JCI23618.
[44] S.J. Poureetezadi, C.N. Cheng, J.M. Chambers, B.E. Drummond, R.A. Wingert, Prostaglandin signaling regulates nephron segment patterning of renal progenitors during zebrafish kidney development, 2016, https://doi.org/10.7554/eLife.17551.001.
[45] R.L. Miyares, V.B. de Rezende, S.A. Farber, Zebrafish yolk lipid processing: a tractable tool for the study of vertebrate lipid transport and metabolism, Dis. Model. Mech. 7 (2014) 915–927, https://doi.org/10.1242/dmm.015800.
[46] D. Fraher, A. Sanigorski, N.A. Mellett, P.J. Meikle, A.J. Sinclair, Y. Gibert, Zebrafish embryonic lipidomic analysis reveals that the yolk cell is metabolically active in processing lipid, Cell Rep. 14 (2016) 1317–1329, https://doi.org/10.1016/j.celrep.2016.01.016.
[47] J.D. Niringiyumukiza, H. Cai, W. Xiang, Prostaglandin E2 involvement in mammalian female fertility: ovulation, fertilization, embryo development and early implantation, Reprod. Biol. Endocrinol. 16 (2018) 43, https://doi.org/10.1186/s12958-018-0359-5.
[48] J. Ke, Y. Yang, Q. Che, F. Jiang, H. Wang, Z. Chen, M. Zhu, H. Tong, H. Zhang, X. Yan, X. Wang, F. Wang, Y. Liu, C. Dai, X. Wan, Prostaglandin E2 (PGE2) promotes proliferation and invasion by enhancing SUMO-1 activity via EP4 receptor in endometrial cancer, Tumor Biol. 37 (2016) 12203–12211, https://doi.org/10.1007/s13277-016-5087-x.
[49] D.F. Legler, M. Bruckner, E. Uetz-von Allmen, P. Krause, Prostaglandin E2 at new glance: novel insights in functional diversity offer therapeutic chances, Int. J. Biochem. Cell Biol. 42 (2010) 198–201, https://doi.org/10.1016/j.biocel.2009.09.015.
[50] P. Kaczynski, S. Bauersachs, E. Goryszewska, M. Baryla, A. Waclawik, Synergistic action of estradiol and PGE2 on endometrial transcriptome in vivo resembles pregnancy effects better than estradiol alone, Biol. Reprod. 104 (2021) 818–834, https://doi.org/10.1093/biolre/ioaa230.
[51] A.N. Marra, B.D. Adeeb, B.E. Chambers, B.E. Drummond, M. Ulrich, A. Addiego, M. Springer, S.J. Poureetezadi, J.M. Chambers, M. Ronshaugen, R.A. Wingert, Prostaglandin signaling regulates renal multiciliated cell specification and maturation, Proc. Natl. Acad. Sci. U. S. A. 116 (2019) 8409–8418, https://doi.org/10.1073/pnas.1813492116.
[52] K.P. Wingert, RA, Molecular mechanisms of podocyte development revealed by zebrafish kidney research, Cell Dev. Biol. 03 (2014), https://doi.org/10.4172/2168-9296.1000138.
[53] Z. Chen, A. Luciani, J.M. Mateos, G. Barmettler, R.H. Giles, S.C.F. Neuhauss, O. Devuyst, Transgenic zebrafish modeling low-molecular-weight proteinuria and lysosomal storage diseases, Kidney Int. 97 (2020) 1150–1163, https://doi.org/10.1016/j.kint.2019.11.016.
[54] A. Majumdar, I.A. Drummond, Podocyte differentiation in the absence of endothelial cells as revealed in the zebrafish avascular mutant, cloche, Dev. Genet. 24 (1999) 220–229, https://doi.org/10.1002/(SICI)1520-6408(1999)24:3/4<220::AID-DVG5>3.0.CO;2-1.
[55] N. Endlich, O. Simon, A. Göpferich, H. Wegner, M.J. Moeller, E. Rumpel, A. M. Kotb, K. Endlich, Two-photon microscopy reveals stationary podocytes in living zebrafish larvae, J. Am. Soc. Nephrol. 25 (2014) 681–686, https://doi.org/10.1681/ASN.2013020178.
[56] K. Ichimura, Y. Fukuyo, T. Nakamura, R. Powell, T. Sakai, R. Janknecht, T. Obara, Developmental localization of nephrin in zebrafish and medaka pronephric glomerulus, J. Histochem. Cytochem. 61 (2013) 313–324, https://doi.org/10.1369/0022155413477115.
[57] T. Müller, E. Rumpel, S. Hradetzky, F. Bollig, H. Wegner, A. Blumenthal, A. Greinacher, K. Endlich, N. Endlich, Non-muscle myosin IIA is required for the development of the zebrafish glomerulus, Kidney Int. 80 (2011) 1055–1063, https://doi.org/10.1038/ki.2011.256.
[58] I.A. Drummond, A. Majumdar, H. Hentschel, M. Elger, L. Solnica-Krezel, A. F. Schier, S.C. Neuhauss, D.L. Stemple, F. Zwartkruis, Z. Rangini, W. Driever, M. C. Fishman, Early development of the zebrafish pronephros and analysis of mutations affecting pronephric function, Development 125 (1998) 4655–4667, https://doi.org/10.1242/dev.125.23.4655.
[59] C. Cianciolo Cosentino, A. Berto, S. Pelletier, M. Hari, J. Loffing, S.C.F. Neuhauss, V. Doye, Moderate nucleoporin 133 deficiency leads to glomerular damage in zebrafish, Sci. Rep. 9 (2019), https://doi.org/10.1038/s41598-019-41202-4.
[60] R. Repetti, N. Majumder, K.C. De Oliveira, J. Meth, T. Yangchen, M. Sharma, T. Srivastava, R. Rohatgi, Unilateral nephrectomy stimulates ERK and is associated with enhanced Na transport, Front. Physiol. 12 (2021) 1–10, https://doi.org/10.3389/fphys.2021.583453.
[61] M. Sharma, R. Sharma, E.T. McCarthy, V.J. Savin, T. Srivastava, Hyperfiltration-associated biomechanical forces in glomerular injury and response: potential role for eicosanoids, Prostaglandins Other Lipid Mediat. 132 (2017) 59–68, https://doi.org/10.1016/j.prostaglandins.2017.01.003.
[62] T. Srivastava, G.E. Celsi, M. Sharma, H. Dai, E.T. McCarthy, M. Ruiz, P.A. Cudmore, U.S. Alon, R. Sharma, V.A. Savin, Fluid flow shear stress over podocytes is increased in the solitary kidney, Nephrol. Dial. Transplant. Off. Publ. Eur. Dial. Transpl. Assoc. - Eur. Ren. Assoc. 29 (2014) 65–72, https://doi.org/10.1093/ndt/gft387.
[63] W. Zhou, F. Hildebrandt, Inducible podocyte injury and proteinuria in transgenic zebrafish, J. Am. Soc. Nephrol. 23 (2012) 1039–1047, https://doi.org/10.1681/ASN.2011080776.
[64] V.L. Hood, Prostaglandins and the Kidney, 1977. www.physiology.org/journal/ajprenal.
[65] M.K. Mansley, C. Niklas, R. Nacken, K. Mandery, H. Glaeser, M.F. Fromm, C. Korbmacher, M. Bertog, Prostaglandin E2 stimulates the epithelial sodium channel (ENaC) in cultured mouse cortical collecting duct cells in an autocrine manner, J. Gen. Physiol. 152 (2020) 1–15, https://doi.org/10.1085/jgp.201912525.
[66] I.J. Chen, S.W. Hee, C.H. Liao, S.Y. Lin, L. Su, C.T. Shun, L.M. Chuang, Targeting the 15-keto-PGE2-PTGR2 axis modulates systemic inflammation and survival in experimental sepsis, Free Radic. Biol. Med. 115 (2018) 113–126, https://doi.org/10.1016/j.freeradbiomed.2017.11.016.
[67] E.J. Lee, S.-J. Kim, Y.-I. Hahn, H.-J. Yoon, B. Han, K. Kim, S. Lee, K.P. Kim, Y. G. Suh, H.-K. Na, Y.-J. Surh, 15-keto prostaglandin E2 suppresses STAT3 signaling and inhibits breast cancer cell growth and progression, Redox Biol. 23 (2019), 101175, https://doi.org/10.1016/j.redox.2019.101175.

[68] B.W. Kim, H.J. Kim, S.-H. Kim, H.J. Baik, M.S. Kang, D.-H. Kim, S.D. Markowitz, S. W. Kang, K.B. Bae, 15-hydroxyprostaglandin dehydrogenase inhibitor prevents contrast-induced acute kidney injury, Ren. Fail. 43 (2021) 168–179, https://doi.org/10.1080/0886022X.2020.1870139.

[69] H.J. Kim, S.H. Kim, M. Kim, H.J. Baik, S.J. Park, M.S. Kang, D.H. Kim, B.W. Kim, S. D. Markowitz, K.B. Bae, Inhibition of 15-PGDH prevents ischemic renal injury by the PGE2/EP4signaling pathway mediating vasodilation, increased renal blood flow, and increased adenosine/A2Areceptors, Am. J. Physiol. - Ren. Physiol. 319 (2020) F1054–F1066, https://doi.org/10.1152/AJPRENAL.00103.2020.

[70] S. Miao, C. Lv, Y. Liu, J. Zhao, T. Li, C. Wang, Y. Xu, X. Wang, X. Xiao, H. Zhang, Pharmacologic blockade of 15-PGDH protects against acute renal injury induced by LPS in mice, Front. Physiol. 11 (2020). https://www.frontiersin.org/articles/10.3389/fphys.2020.00138.

[71] S. Sakuma, Y. Fujimoto, H. Nakagawa, S. Hachiki, H. Nishida, T. Fujita, Effect of 13-hydroperoxyoctadecadienoic acid on 15-hydroxy prostaglandin dehydrogenase activity in rabbit kidney cortex, Prostaglandins 46 (1993) 157–165, https://doi.org/10.1016/0090-6980(93)90041-5.

[72] S. Sakuma, Y. Fujimoto, E. Hikita, Y. Okano, I. Yamamoto, T. Fujita, Effects of metal ions on 15-hydroxy prostaglandin dehydrogenase activity in rabbit kidney cortex, Prostaglandins 40 (1990) 507–514, https://doi.org/10.1016/0090-6980(90)90112-9.

[73] M.Y. Tsai, S. Einzig, Prostaglandin catabolism in fetal and maternal tissues — a study of 15-hydroxyprostaglandin dehydrogenase and Δ13 reductase with specific assay methods, prostaglandins, Leukot. Essent. Fat. Acids. 38 (1989) 25–30, https://doi.org/10.1016/0952-3278(89)90143-9.

[74] W. Ye, H. Zhang, E. Hillas, D.E. Kohan, R.L. Miller, R.D. Nelson, M. Honeggar, T. Yang, Expression and function of COX isoforms in renal medulla: evidence for regulation of salt sensitivity and blood pressure, Am. J. Physiol. Renal Physiol. 290 (2006) F542–F549, https://doi.org/10.1152/ajprenal.00232.2005.

[75] J. Wang, M. Liu, X. Zhang, G. Yang, L. Chen, Physiological and pathophysiological implications of PGE2 and the PGE2 synthases in the kidney, Prostaglandins Other Lipid Mediat. 134 (2018) 1–6, https://doi.org/10.1016/j.prostaglandins.2017.10.006.

[76] M. Imanishi, Y. Abe, T. Okahara, T. Yukimura, K. Yamamoto, Effects of prostaglandin I2 and E2 on renal hemodynamics and function and renin release, Jpn. Circ. J. 44 (1980) 875–882, https://doi.org/10.1253/jcj.44.875.

[77] B. Bądzyńska, J. Sadowski, Renal hemodynamic responses to intrarenal infusion of acetylcholine: comparison with effects of PGE2 and NO donor, Kidney Int. 69 (2006) 1774–1779, https://doi.org/10.1038/sj.ki.5000338.

[78] L.P. Audoly, S.L. Tilley, J. Goulet, M. Key, M. Nguyen, J.L. Stock, J.D. McNeish, B. H. Koller, T.M. Coffman, Identification of specific EP receptors responsible for the hemodynamic effects of PGE2, Am. J. Physiol. - Hear. Circ. Physiol. 277 (1999), https://doi.org/10.1152/ajpheart.1999.277.3.h924.

[79] L.P. Audoly, X. Ruan, V.A. Wagner, J.L. Goulet, S.L. Tilley, B.H. Koller, T. M. Coffman, W.J. Arendshorst, P. Laurent, X. Ruan, J.L. Goulet, S.L. Tilley, H. Beverly, T.M. Coffman, W.J. Arendshorst, V.A. Wag, in: Role of EP 2 and EP 3 PGE 2 Receptors in Control of Murine Renal Hemodynamics, 2022, pp. 327–333.

[80] P. Aleström, L. D'Angelo, P.J. Midtlyng, D.F. Schorderet, S. Schulte-Merker, F. Sohm, S. Warner, Zebrafish: housing and husbandry recommendations, Lab. Anim. 54 (2019) 213–224, https://doi.org/10.1177/0023677219869037.

[81] B. Perner, C. Englert, F. Bollig, The wilms tumor genes wt1a and wt1b control different steps during formation of the zebrafish pronephros, Dev. Biol. (2007), https://doi.org/10.1016/j.ydbio.2007.06.022.

[82] M.A. Saleem, M.J. O'Hare, J. Reiser, R.J. Coward, C.D. Inward, T. Farren, C. Y. Xing, L. Ni, P.W. Mathieson, P. Mundel, A conditionally immortalized human podocyte cell line demonstrating nephrin and podocin expression, J. Am. Soc. Nephrol. 13 (2002) 630–638, https://doi.org/10.1681/ASN.V133630.